J Digit Imaging (2014) 27:610–624
DOI 10.1007/s10278-014-9704-1

# Entropy-Based Straight Kernel Filter for Echocardiography Image Denoising

**S. Rajalaxmi · S. Nirmala**

Published online: 17 May 2014


**Abstract** A new filter has been proposed with the aim of eliminating speckle noise from 2D echocardiography images. This speckle noise has to be eliminated to avoid the pseudo prediction of the underlying anatomical facts. The proposed filter uses entropy parameter to measure the disorganized occurrence of noise pixel in each row and column and to increase the image visibility. Straight kernels with 3 pixels each are chosen for the filtering process, and the filter is slided over the image to eliminate speckle. The peak signal-to-noise ratio (PSNR) is obtained in the range of 147 dB, and the root mean square error (RMSE) is very low of approximately 0.15. The proposed filter is implemented on 36 echocardiography images, and the filter has the competence to illuminate the actual anatomical facts without degrading the edges.

**Keywords** Echocardiography · Speckle noise · Kernel · Entropy · Additive noise · Variance

## Introduction

Ultrasound has proven its importance to assess the heart diseases in the form of echocardiography. This is one of the most widely used diagnostic tests in cardiology, as it is non-invasive, nonionizing, real time, portable, and low cost in nature. But the ultrasound images are affected by artifacts called speckle, produced by interfering echoes. This multiplicative-natured speckle noise degrades spatial and contrast resolution and makes the underlying anatomy incomprehensible [1]. This curtails human interpretation of diagnosis and computer-assisted detection techniques. Since speckle is a major limitation of ultrasound images, reducing or eliminating speckle is of great importance in the processing of ultrasound images and improving its visibility. Image visibility is dependent on pixels with higher intensity levels and their distribution [2].

A number of filtering schemes are available in the literature which have their own uniqueness and setbacks. The filtering techniques established so far include filters in spatial domain and frequency domain. The frequency domain filters divide the whole image into sub-bands and implement thresholds for the bands for speckle removal. The wavelet transform techniques are efficient as they capture the energy of the signal in few transform coefficients. The spatial domain filters utilize a fixed moving window to replace the noise pixels based on the statistical properties of the image. The difficulty arises in the selection of weighting coefficients and window size for the varying properties of the image. The most predominant median filter chooses a sliding window for speckle reduction with duration of less than half the window size [3]. The degree of smoothing depends on the window size, and high-frequency signals are also removed during speckle filtering which causes edge blurring. When the speckle size is larger than the window size, speckle remains as an artifact. Many approaches in the literature take the advantage of converting the multiplicative model of speckle noise into additive noise by performing logarithmic transformation. The log transform eliminates the phase relationship between the transducer element outputs [4, 5]. The samples of additive noise are mutually uncorrelated, and they obey Gaussian distribution; hence, the noise can be termed as additive white Gaussian noise [6]. Hence, the filters which suppress additive noise can be taken under

S. Rajalaxmi (✉)
Electrical and Electronics Engineering, Paavai Engineering College, NH-7 Pachal, Namakkal 637 018, Tamil Nadu, India
e-mail: rajalaxmisakthivelpec@paavai.edu.in

S. Nirmala
Electronics and Communication Engineering, Muthayammal Engineering College, Rasipuram, Namakkal 637 408, Tamil Nadu, India
e-mail: nirmala.ramkamal@gmail.com

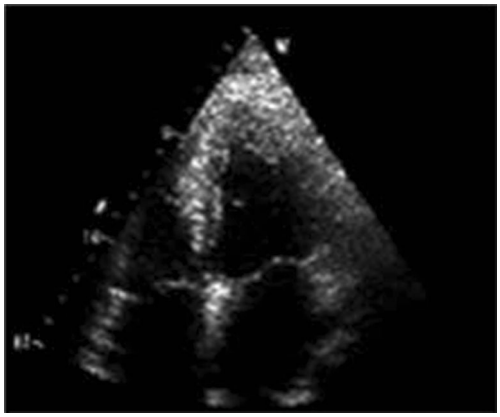

**Fig. 1** Speckle noise sample

consideration for comparative assessment. Spatial-domain filters such as mean filter, tri-state median filter, alpha-trimmed mean filter, Wiener filter, anisotropic diffusion filter, total variation filter, Lee filter, Frost filter, bilateral filter, and non-local means filter are in literature for suppression of additive white Gaussian noise [7–16]. All the abovementioned filters possess mathematical simplicity but include blurring effect, instability due to numerous iterations and deterioration of noise-free pixels. The circular spatial filter is suitable for high noise variance conditions [17]. The circular spatial filter uses a circular window, whose weights are derived from spatial distance and gray level distance. The circular spatial filter uses only the distance metrics, and it does not consider other image statistics. This filter does not perform well under low noise conditions. The wavelet-domain filters, namely, Visu Shrink, Sure Shrink, Bayes Shrink, Neigh Shrink, and Smooth Shrink [18–24] are proposed to suppress the additive noise effectively. The wavelet thresholding methods need to calculate different weights in a local window to distinguish the signal and noise coefficients. The wavelet transform techniques are application specific and suffer from contrast degradation of the output image [25]. Also, the wavelet domain filters suffer from the drawback of discarding some of the useful information needed for study of the anatomical details.

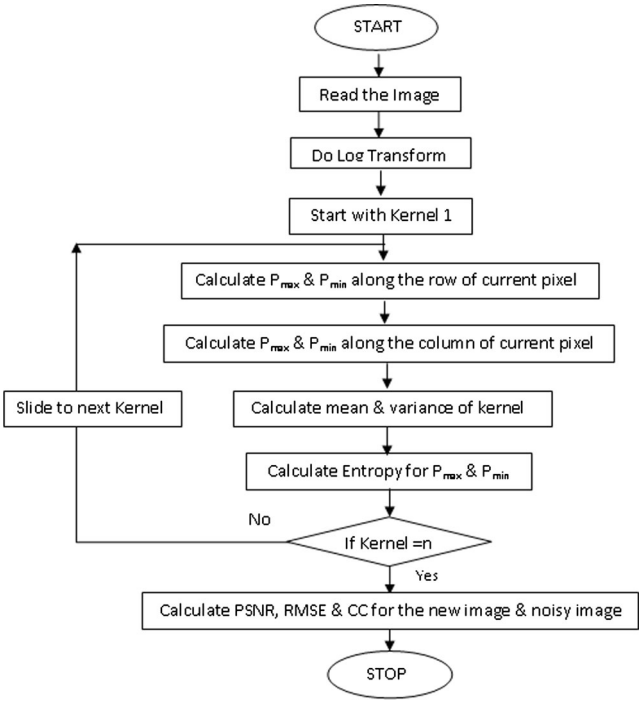


**Fig. 3** Flowchart of the proposed filter

The new entropy-based straight kernel filter has been designed by considering the setbacks of the most renowned spatial domain filters in the literature and has aimed to produce a noise-free output. The filter is adaptable for all noise conditions and concentrates on retaining the intricate anatomical facts of the image. The filter uses a standard straight kernel which considers the variance, mean, and entropy in a constrained scope. The entropy parameter utilized in the filter aids in improving the image visibility, which is always poor in ultrasound images due to improper reception of echoes [26]. The foremost requirement of diagnosis from echocardiography images lies in the identification of the heart walls and defects in the left ventricle of the heart. The proposed filter satisfies the needs of enhancing the edges and noise removal, which will prove to be a quantitative aid for the diagnosis of diseases related to heart.

**Fig. 2** Noise intensity profile

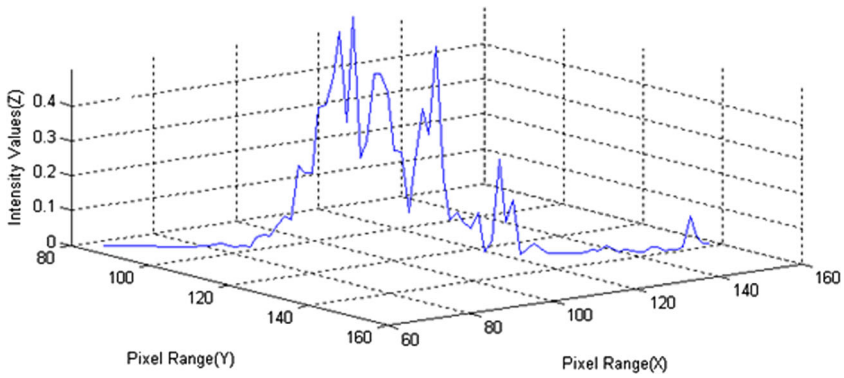

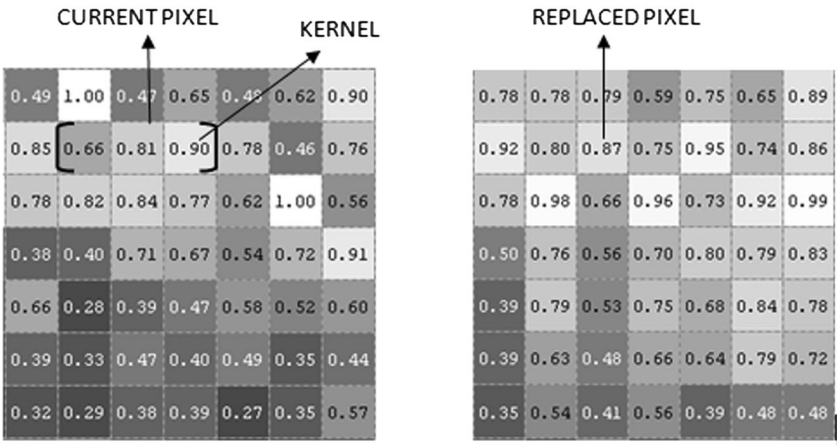


**Fig. 4** Straight kernel filter with sample pixel values

The work has been structured as follows: "Ultrasound Imaging and Speckle Noise," section, "Proposed Filter" section which defines the image fidelity criteria and their need, "Results and Discussion" which describes the features of the new proposed filter and experimental results for the proposed system, and finally, "Conclusion" which concludes the paper.

## Ultrasound Imaging and Speckle Noise

Speckle in ultrasound image is seen as a granular structure. This is caused by the constructive and destructive coherent interferences of backscattered echoes from the scatterers that are typically much smaller than the spatial resolution of medical ultrasound system. The speckle accompanies all coherent imaging techniques, namely LASER, SONAR, and synthetic aperture radar imagery (SAR) [27]. They are produced by interfering echoes of a transmitted wave form, which emanate from heterogeneities of the objects being interrogated. In this case, there is a possibility that a dark spot could be interpreted by a medical doctor as corresponding to a blood vessel or a cyst with relatively low reflectivity, while in fact, it might be merely caused by echoes compensating each other at opposite phases [28].

Speckle pattern is a form of multiplicative noise because speckle noise is a signal-dependent noise; if the image pixel magnitude is high, then the noise is also high. It depends on the structure of imaged tissue and various imaging parameters. As a result, image processing methods for curbing the speckle noise have established constructive for enhancing image quality and, thereby, escalating the diagnostic potential of medical ultrasound. The model of speckle [29] is given by

$$g(m,n) = f(m,n).u(m,n) + \zeta(m,n) \tag{2.1}$$

where, $g\ (m,\ n)$ is the observed image, $u\ (m,\ n)$ is the multiplicative component, and $\zeta\ (m,n)$ is the additive component of the speckle noise. Here, $m$ and $n$ denote the axial and lateral indices of the image samples.

The noise level in an echocardiography image is the amount of speckle noise distribution in terms of variance. The noise intensity differs from pixel to pixel, depending on the echo scatterers. This noise distribution can be seen with the help of noise intensity profile for any specific pixel range. Figures 1 and 2 show apical four-chamber view of a normal heart with speckle noise level of 0.06 and its corresponding noise intensity profile. It is a 3D plot with intensity values along z axis versus pixel range along x and y axes. The

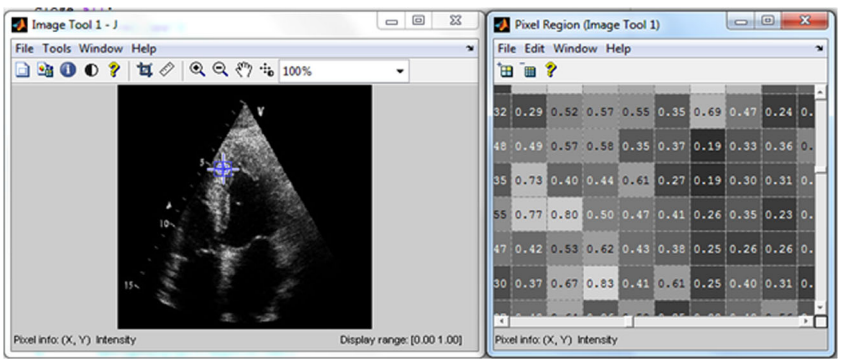


**Fig. 5** Sample pixel range before application of proposed filter

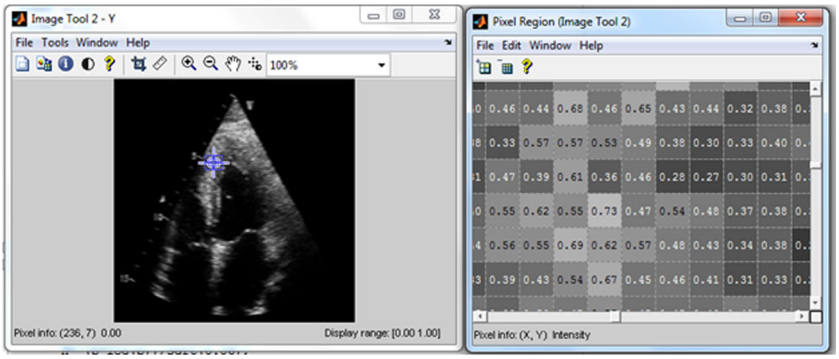


**Fig. 6** Sample pixel range after application of proposed filter

intensity profile clearly portrays the presence of noise by the sharp, closer, spikes. This noise present in the image has to be removed in order to enhance the clarity of visualization and thus proper study of features from the image.

## Image Metrics

Objective image quality measures play an imperative role in various image processing applications. The mathematically defined image quality measures include mean square error (MSE), root mean square error (RMSE), peak signal-to-noise ratio (PSNR), and correlation coefficient (CC). The image quality measures are very attractive as they are very easy to compute and have low computational complexity. The quality measures are independent of the viewing conditions and individual observers [30]. The image quality measures predicted between the original image $f(m, n)$, and the reconstructed image $g(m, n)$ is given below.

## Mean Square Error

The mean square error between the original image $f(m, n)$ and the reconstructed image g (m, n) is given by

$$\mathrm{MSE} = \frac{1}{M \times N} \sum_{m=1}^{M} \sum_{n=1}^{N} (f(m,n) - g(m,n)) \tag{2.2}$$

where $M \times N$ represents the size of the image. MSE measures the average of the squares of the errors. The error is the amount by which the value implied by the estimator differs from the quantity to be estimated. The mean square error is a very useful measure of the energy lost in the lossy compression of the image $f(m, n)$. A very small MSE can be taken to mean that the image is very close to the original.

## Root Mean Square Error

The root mean square error (RMSE) is the square root of mean square error, and the value should be minimal for better quality of image. The RMSE value can be calculated as,

$$\mathrm{RMSE} = \sqrt{\mathrm{MSE}} \tag{2.3}$$

## Peak Signal-to-Noise Ratio

Peak signal-to-noise ratio (PSNR) is a subjective qualitative measurement of distortion. The PSNR measure is superior to other measures such as signal-to-noise ratio, as it uses a constant value in which to compare the noise against instead of a fluctuating signal as in signal-to-noise ratio. The measure of PSNR can be treated as a more significant and irrefutable measure as it depicts the image quality more astoundingly. It is measured in decibels (dB). The value of PSNR can be obtained using,

$$\mathrm{PSNR} = 10 \log \frac{255^2}{\mathrm{MSE}} \tag{2.4}$$

**Table 1** Simulated results for the proposed filter

| Proposed filter with different noise levels | PSNR (dB) | RMSE | CC |
|---|---|---|---|
| Linear summation with maximum intensity pixel | | | |
| 0.03 | 147.8310 | 0.1572 | 0.935 |
| 0.04 | 147.8088 | 0.1574 | 0.954 |
| 0.05 | 147.7607 | 0.1577 | 0.956 |
| 0.06 | 147.8030 | 0.1574 | 0.964 |
| Linear summation with minimum intensity pixel | | | |
| 0.03 | 147.8093 | 0.1574 | 0.943 |
| 0.04 | 147.8321 | 0.1572 | 0.955 |
| 0.05 | 147.7668 | 0.1577 | 0.961 |
| 0.06 | 147.6965 | 0.1583 | 0.959 |

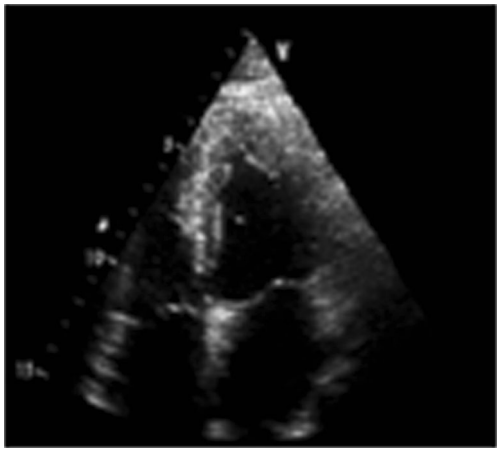

**Fig. 7** Apical four-chamber view with 0.03 noise level

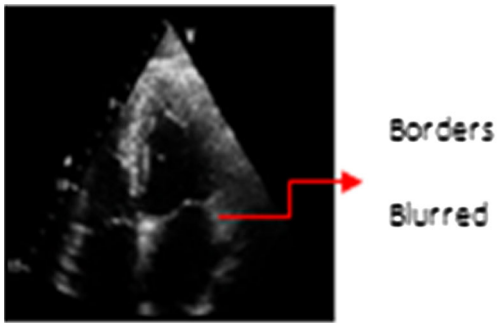


**Fig. 9** Apical four-chamber view with 0.04 noise level

### Correlation Coefficient

Correlation indicates the strength and direction of linear relationship between two images, and its value lies between +1 to −1. The correlation is 1 in the case of an increasing linear relationship, −1 in the case of a decreasing linear relationship, and some value in between for all the other cases, including the degree of linear dependence between the two images. The closer the coefficient is to either −1 or +1, the stronger the correlation between the images. The value of correlation coefficient (CC) can be calculated using,

$$\mathrm{CC} = \frac{\sum \left(f(m,n)-f^{'}(m,n)\right)-\left(f^{'}(m,n)-g(m,n)\right)}{\sqrt{\sum \left(f(m,n)-f^{'}(m,n)\right)^{2}\sum \left(g(m,n)-g^{'}(m,n)\right)^{2}}} \tag{2.5}$$

where $f'(m,n)$ is the mean of the original image and $g'(m,n)$ is the mean of the denoised image.

### Proposed Filter

Speckle noise in the ultrasound images may lead to the misinterpretation of high- and low-contrast portions. The steps carried out in the proposed filter are shown in the flowchart (Fig. 3). The entropy-based straight kernel filter is proposed with the advent of improving the image visibility of the ultrasound image, thereby revealing the originality of the pixels from noise.

### Straight Kernel

The name straight kernel refers to a straight (1×3) window, where 1 and 3 are the axial and lateral indices of the image sample.

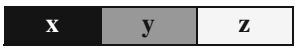


This is a straight kernel with pixel elements x, y, and z. The filter measures the signal content from the noise in each straight kernel and replaces the pixels with noise-free intensity. For each kernel, variance and mean are evaluated and combined with entropy. This improves the visibility of edges present in the image. The process is repeated for all the kernels in the image, and the quality measures are evaluated for comparison.

**Fig. 8** Noise intensity profile

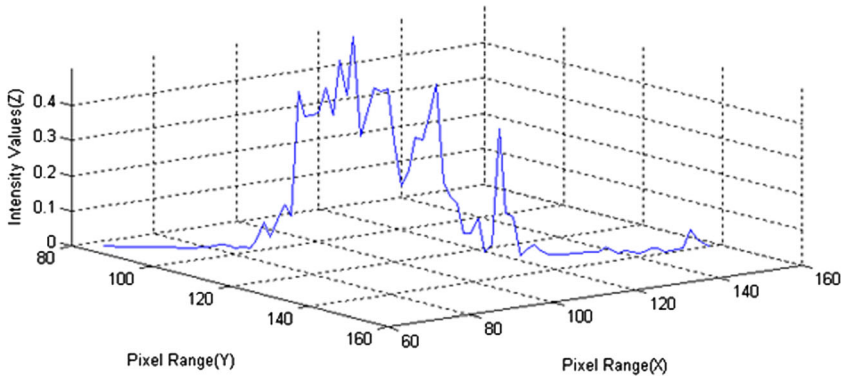

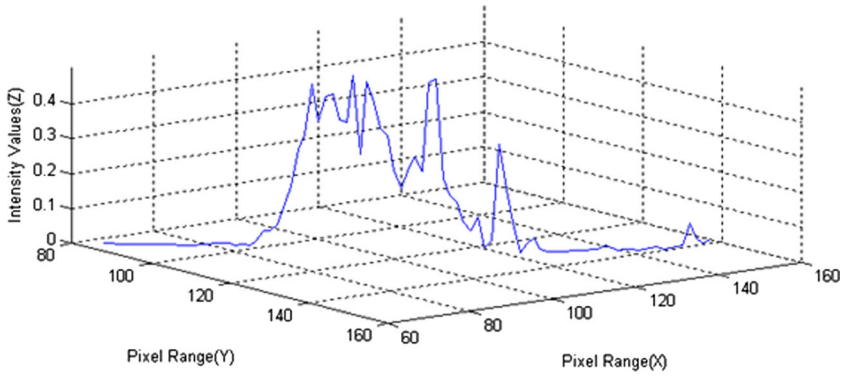


**Fig. 10** Noise intensity profile

Filter Function

The proposed filter checks the unsystematic noise occurrence in the image and eliminates the noise by shifting in a linear fashion. Entropy is a statistical measure of randomness that can be used to characterize the texture of the input image. Each pixel is assumed to be the center of the neighboring pixels, and that pixel is replaced by performing a linear summation with a probability check of noise in each row and column. It is estimated that always a pixel affected by noise will be predicted as a maximum intensity pixel or a minimum intensity pixel. The probability check of maximum or minimum intensity pixel is utilized for entropy calculation. The concept of entropy is utilized to enhance the luminance of each pixel. A process of linear regression combined with a measure of randomness of noise episode is performed to modify each pixel. The proposed filter can be implemented with following equations.

$$\text{mean} = \frac{1}{K}\left[\sum_{j=j-1}^{j+1} J(i,j)\right] \tag{3.1}$$

where $K$ indicates the kernel size, which is 3 in the case of the proposed work. $J(i, j)$ represents the pixels in the kernel. The variance of the proposed filter can be calculated as,

$$\sigma_k^2 = \frac{1}{K-1}\left[\sum_{j=j-1}^{j+1} (J(i,j)-\text{mean})^2\right] \tag{3.2}$$

where $\sigma_k{}^2$ is the variance of the kernel. The variance is estimated to find the spread out of noise in the respective kernel. These Eqs. (3.1) and (3.2) represent the statistical measures needed to find the distribution of noise in the kernel.

Probability and Modified Shannon Entropy

The probability of the occurrence of maximum intensity pixel along the row and column of the current pixel is found using Eq. (3.3), and that for minimum intensity pixel is calculated using Eq. (3.4).

$$P_{\max} = \frac{1}{2}\left[\frac{\max_i}{m} + \frac{\max_j}{n}\right] \tag{3.3}$$

$$P_{\min} = \frac{1}{2}\left[\frac{\min_i}{m} + \frac{\min_j}{n}\right] \tag{3.4}$$

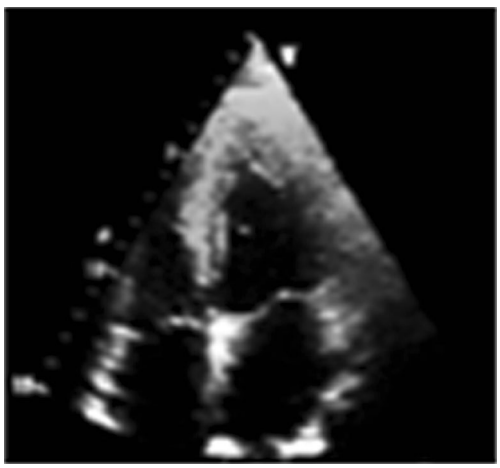

**Fig. 11** Output of the proposed filter with noise level of 0.03 for $P_{\min}$

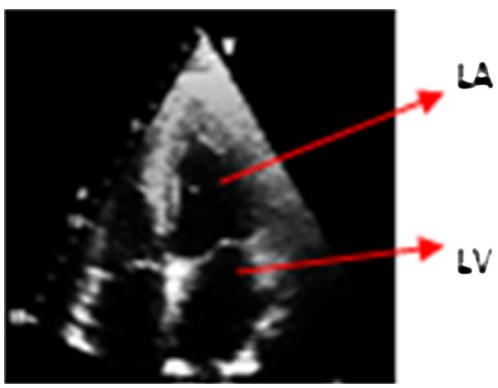


**Fig. 12** Output of the proposed filter with noise level of 0.03 for $P_{\max}$

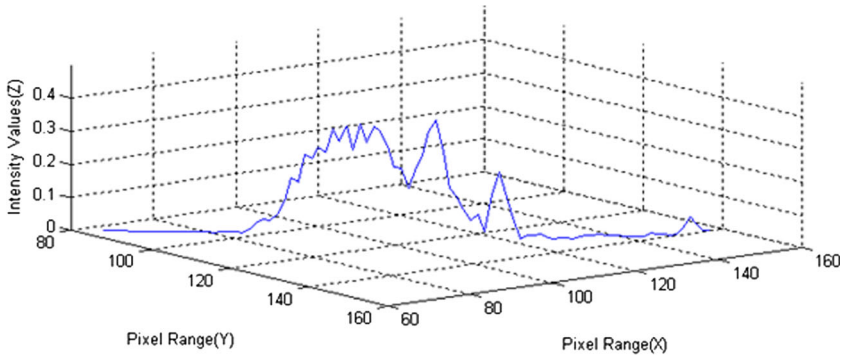


**Fig. 13** Noise intensity profile

where $m$ and $n$ represent the number of elements along the row and column, respectively, $\max_i$ and $\min_i$ are the maximum and minimum intensity pixels along row ($i$), and $\max_j$ and $\min_j$ are the maximum and minimum intensity pixels along column ($j$). The value 2 indicates the two vector consideration.Equations (3.5) and (3.6) represent a modified Shannon entropy equation. This utilizes the probability values found using Eqs. (3.3) and (3.4).

$$H_{\max} = -\frac{1}{\sigma}(P_{\max} \times \log_2 P_{\max}) \tag{3.5}$$

$$H_{\min} = -\frac{1}{\sigma}(P_{\min} \times \log_2 P_{\min}) \tag{3.6}$$

where $\sigma$ indicates the standard deviation of the noise level in the image. The modified entropy is determined using the probability of maximum intensity pixel $P_{\max}$ and the minimum intensity pixel $P_{\min}$. This provides a measure of noise that is distributed in the respective kernel. The entropy function measures the random existence of noise in each kernel with respect to the standard deviation $\sigma$.

The proposed filter can then be implemented using the following equation. Eqs. (3.7) and (3.8) represent the proposed filter equations with $J(i, j)$ as the current pixel of the chosen kernel.

$$J(i,j) = \frac{1}{e^{\log\sigma_k^2} + H_{\max}} \left[ \sum_{j=j-1, j\neq j}^{j+1} J(i,j) \right] \tag{3.7}$$

$$J(i,j) = \frac{1}{e^{\log\sigma_k^2} + H_{\min}} \left[ \sum_{j=j-1, j\neq j}^{j+1} J(i,j) \right] \tag{3.8}$$

The kernel selected is a straight 3 elements kernel. The center pixel is the current pixel that is to be replaced by the linear summation of the neighborhood pixels (Fig. 4). Speckle noise is a signal-dependent noise which can be modeled by the exponential function. The use of the exponential function in the kernel combined with logarithmic function of kernel variance $\sigma_k^2$ provides a proportionate noise removal in the respective kernel. This function, when it is pooled with the modified Shannon entropy function $H_{\max}$ or $H_{\min}$ (modified Shannon entropy equation), explores the kernel signal content from noise and improves image visibility. The proposed filter has the ability to remove the speckle noise, since nearby points

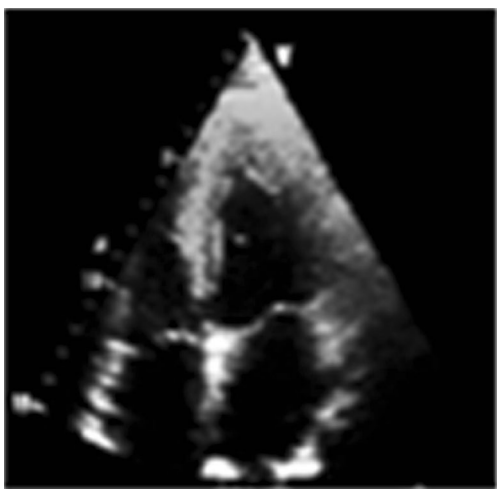

**Fig. 14** Output of the proposed filter with noise level of 0.04 for $P_{\min}$

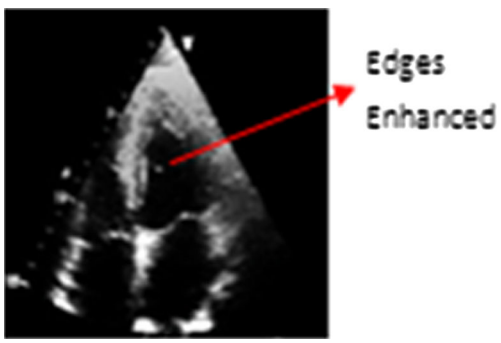


**Fig. 15** Output of the proposed filter with noise level of 0.04 for $P_{\max}$

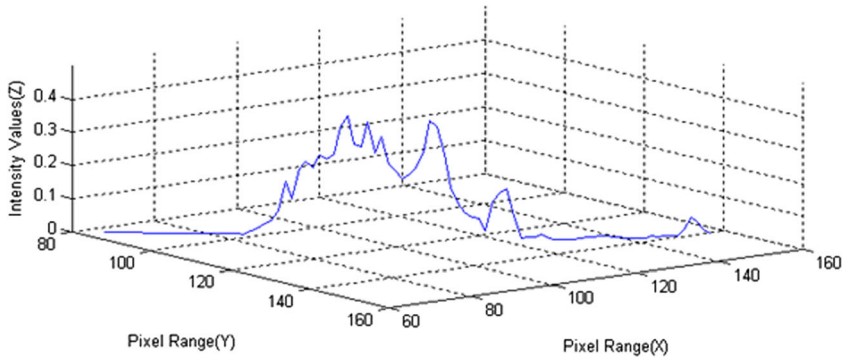


**Fig. 16** Noise intensity profile

compute very nearly the same underlying value, and entropy estimation can reduce the level of noise without biasing the value obtained. The filtering technique manages to provide smoothing without loss of resolution. The entropy parameter also has the significance of improving the luminance of the dull regions of the ultrasound image, which may be lost due to improper echoes. The filter mainly quantifies the luminance of the dead zone pixels and suppresses the dominating noise pixels. The hypothesis of noise removal is that a noise pixel has either a maximum or minimum value that always differs from the neighboring linear elements. The tarnished pixel is replaced by finding the probability of the maximum or minimum row pixel and column pixel with an attempt of removing noise from the current pixel.

Figures 5 and 6 represent the range of pixel values from the ultrasound image used for analysis. The pixel region shown is a small portion of the image used for illustration of the proposed filter.

Figure 5 indicates the pixel values, before the application of the proposed filter. The values are randomly distributed with mixture of noisy pixels. After the application of the proposed filter, the image is smoothened with the elimination of noisy pixels. This is illustrated in Fig. 6.

Figure 5 shows the range of pixel values after the filter application. It is observed that Fig. 6 shows that the image is smoothened with a uniform distribution of pixel range, whereas Fig. 5 shows the nonuniform distribution of noise. This can be enunciated with the pixel value allocation.

## Results and Discussion

The performance of the proposed filter has been analyzed using different noise levels with various parameters which are listed in Table 1. It shows the simulated results for four levels of speckle noise, and the proposed filter can perform better for higher levels of noise also. The proposed filter maintains a constant for changes in the noise level.

The raw images that are considered for the simulation purpose are obtained from GE Vivid 7 Dimension Ultrasound machine. The echocardiography images used are apical four-chamber view and parasternal short axis view images. A total of 36 different frame images are used to substantiate the quality of the proposed filter, and the results for one such frame is presented in this paper. The simulations of these echocardiographic images were performed in Matlab 7, on a

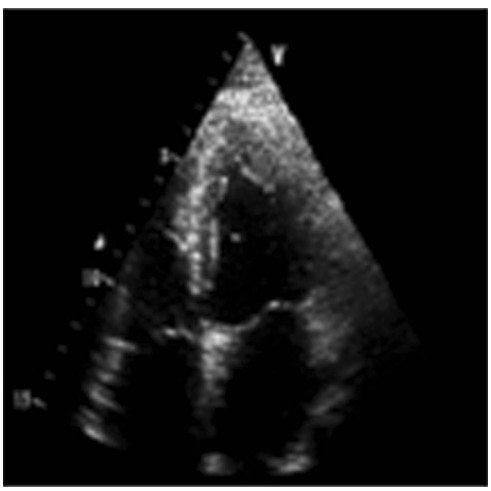

**Fig. 17** Apical four-chamber views of heart with noise level 0.05

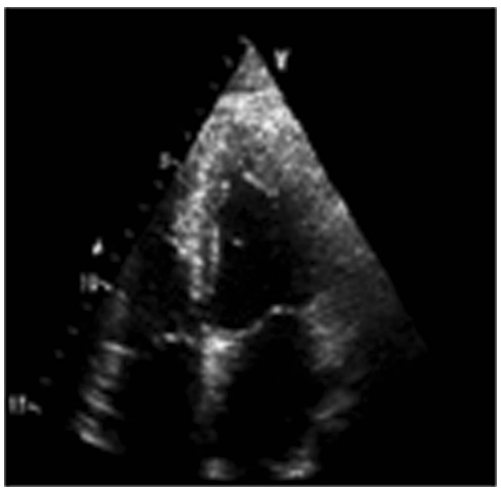

**Fig. 18** Apical four-chamber views of heart with noise level 0.06

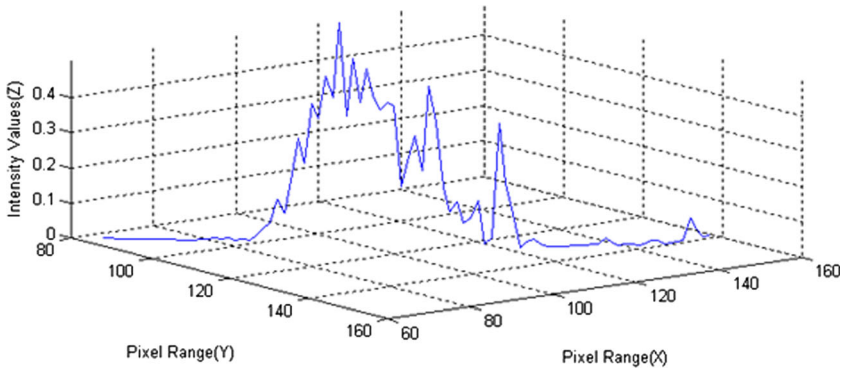


**Fig. 19** Noise profile for 0.05

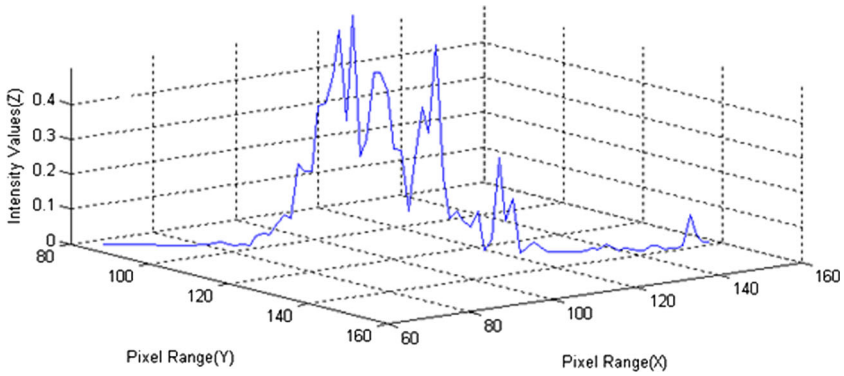


**Fig. 20** Noise profile for 0.06

personal computer with Intel Core 2 Duo processor, 2.93 GHz, 2 Gb random-access memory (RAM).

Figures 7 and 9 show the apical four-chamber views of normal heart with a noise level of 0.03 and 0.04, respectively. The original input images have the drawback of poor clarity in the heart walls, which play a significant role in the diagnosis of heart diseases. The noise intensity profile of the input images is shown in Figs. 8 and 10, respectively. The spiky portions in the intensity profile enunciate the density of noise in the image (Figs. 9 and 10).

This problem can be eliminated using the proposed filter which is shown in Figs. 11 and 12. It shows the output of the proposed filter with probability minimum and maximum intensity pixel considered, respectively, for noise level 0.03. The

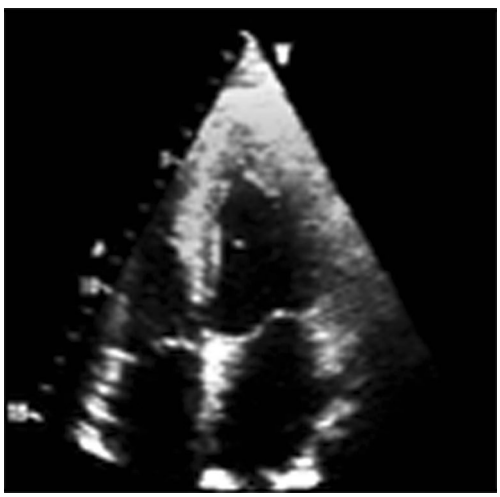

**Fig. 21** Output of the proposed filter for noise level 0.05 ($P_{\min}$)

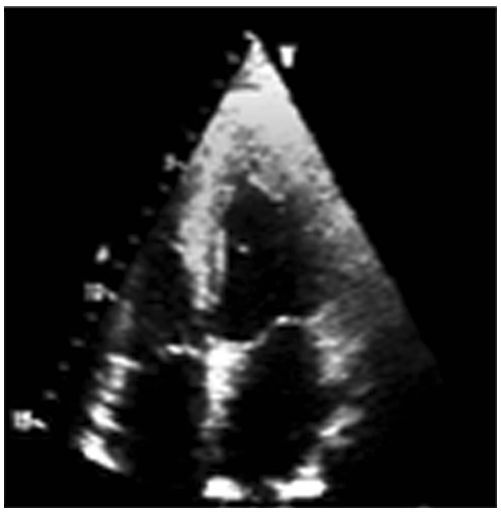

**Fig. 22** Output of the proposed filter for noise level 0.05 ($P_{\max}$ )

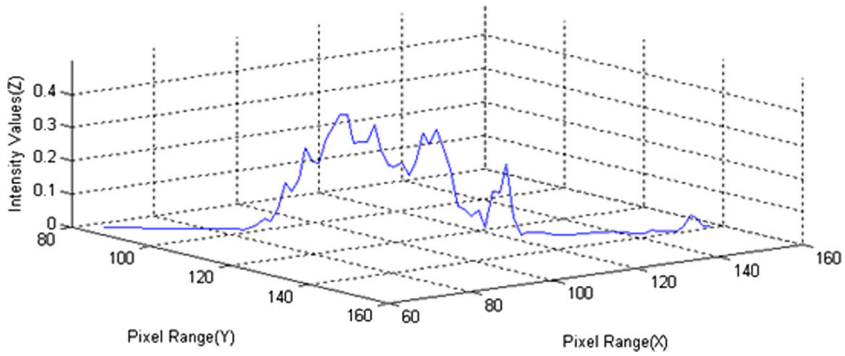


**Fig. 23** Noise intensity profile

change over from the input image with noise can be witnessed clearly. The output images show a very good clarity with enhanced edges and good image visibility. The four chambers of the heart can be seen with good contrast in the gray scale. Figure 13 shows the intensity profile of the output image. The spiky regions present in the intensity profile of the input image are smoothened without degrading its anatomical facts.

Figures 14 and 15 show the output of the proposed filter with probability minimum and maximum intensity pixel considered, respectively, with the noise level 0.04. This clearly provides evidence that as the noise level increases, there is no degradation of the filter performance. The raw image with speckle noise shows that the lower parts of the left ventricle (LV) and left atrium (LA) are completely distorted. This left ventricle, which takes the prevailing responsibility in the diagnosis of many critical diseases, is illuminated and enhanced with the help of the entropy-based straight kernel filter. The filter has clearly shown a bifurcation between the four chambers and is best suitable for diagnosis at both systolic and diastolic periods. The noise intensity profile for the output of the proposed filter is shown in (Fig. 16).

The results shown in Figs. 17, 18, 19, 20, 21, 22, 23, 24, 25, and 26 illustrate the performance of the filter for higher levels of noise. Figures 17 and 18 show the apical four-chamber views of a normal heart with a noise level of 0.05 and 0.06 variance, respectively.

Figures 21 and 22 explain the output of the proposed filter with probability minimum and maximum intensity pixel considered, respectively, for noise level of 0.05. Figures 24 and 25 show the output of the proposed filter with probability minimum and maximum intensity pixel considered, respectively, for noise level of 0.06.

All the outputs presented above prove that the four chambers of the heart are best visualized and help in presenting the anatomical facts more evidently. This may be very helpful in elucidating the area of the chambers, thickness of the heart wall, and blocks if any for the blood passage. The proposed filter is very useful in diagnosing aortic stenosis and hypertrophic cardiomyopathy. The parasternal short axis view for aortic stenosis and apical four-chamber view for hypertrophic cardiomyopathy are shown below with the results of speckle denoising using the proposed filter.

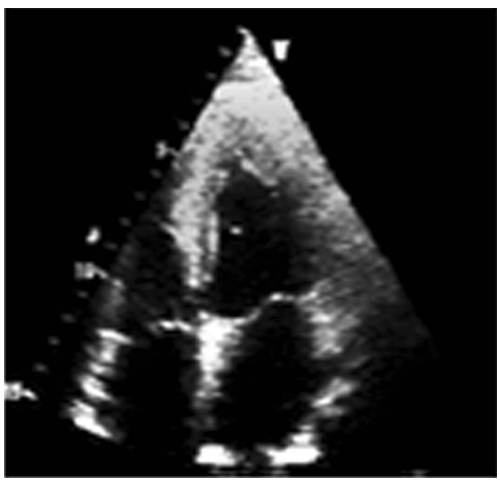

**Fig. 24** Output of the proposed filter for noise level 0.06 ($P_{min}$)

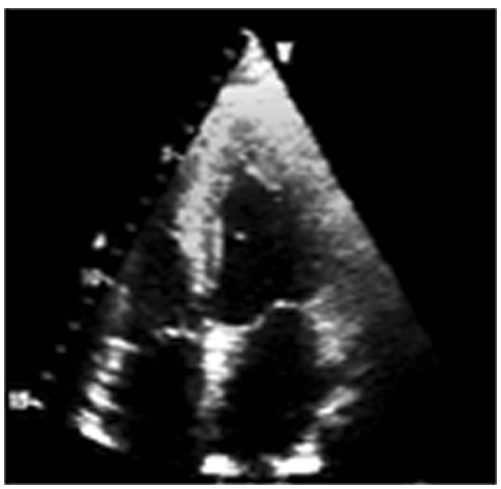

**Fig. 25** Output of the proposed filter for noise level 0.06 ($P_{max}$)

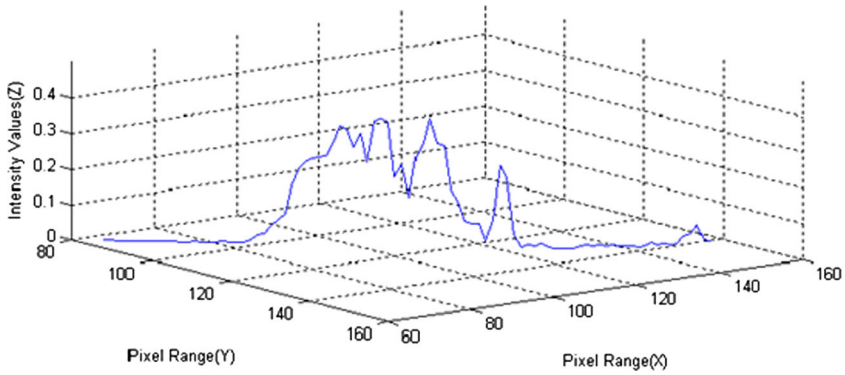


**Fig. 26** Noise intensity profile

Figures 27 and 28 show the apical four-chamber views of the heart with hypertrophic cardiomyopathy with a noise level of 0.04 and its corresponding denoised image, respectively. The myocardium thickness in the case of hypertrophic cardiomyopathy is also effectively elucidated using the proposed filter. The speckle noise has the property of scattering the gray level intensity randomly, which may have the possibility of being misinterpreted as block in blood vessels. Hence, speckle noise removal takes a major role in ultrasound images, for proper analysis of the features present in the image.

Figures 29 and 30 show the parasternal short axis views of the heart with aortic stenosis with a noise level of 0.04 and its corresponding denoised image, respectively. The aortic valve and the mitral valve closed due to aortic stenosis are very clearly out skirted using the proposed filter. The proposed filter will act as a preprocessing step for the image segmentation, which can be used for the diagnosis of hypertrophic cardiomyopathy and aortic stenosis. The heart muscle that is very much thickened in the case of hypertrophic cardiomyopathy can be clearly envisaged, which may be beneficial for future reference and treatments. In the case of aortic stenosis, the aortic and mitral valves are almost closed which in turn reduces the blood outlet and thickens the left ventricle. This is also best witnessed using the proposed filter. Hence, the proposed filter is suitable in speckle denoising the echocardiograms in all the required diagnostic views, namely apical four-chamber view, parasternal short and long axis view, and subcostal chamber view.


**Fig. 27** Apical four-chamber view of heart with hypertrophic cardiomyopathy for noise level of 0.04

## Comparison of the Proposed Filter with Circular Spatial Filter and Bayes Function Filter

The proposed filter is compared with two known spatial domain and frequency domain filters namely, circular spatial filter and wavelet filter with Bayes function. The circular spatial filter is a spatial domain filter, and it uses a circular filter to eliminate speckle noise. The window weights are calculated based on spatial distance and gray level distance. The circular filter has failed to consider other image statistics, namely, mean, variance, and entropy. This filter does not perform well under low noise conditions. The wavelet filter is a frequency domain filter, and it uses wavelet coefficients to remove speckle noise. The weighted variance is calculated from the weights of a local window, and the current coefficient is calculated from the vertical neighbors. Hence, this becomes a tedious procedure to calculate weights, which may be helpful in distinguishing the signal and noise coefficients. These drawbacks have been overcome with the help of the proposed filter, which has eliminated the speckle noise by incorporating

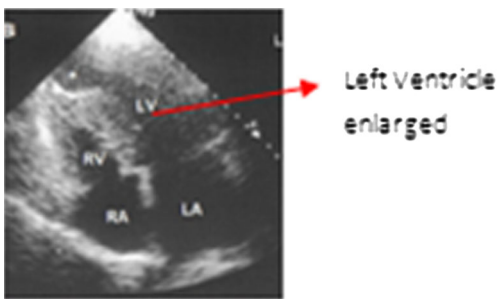


**Fig. 28** Output of the proposed filter

**Fig. 29** Parasternal short axis view of heart with aortic stenosis for noise level of 0.04

**Table 2** Comparison with circular spatial filter and wavelet filter using Bayes function

| Noise level | Image quality | Proposed filter | Circular spatial filter | Wavelet (Bayes) |
|---|---|---|---|---|
| 0.03 | PSNR (dB) | 147.8310 | 71.221 | 65.453 |
| | RMSE | 0.1572 | 8.002 | 8.256 |
| | CC | 0.935 | 0.868 | 0.775 |
| 0.04 | PSNR (dB) | 147.8088 | 71.972 | 64.332 |
| | RMSE | 0.1574 | 7.982 | 8.478 |
| | CC | 0.954 | 0.855 | 0.765 |
| 0.05 | PSNR (dB) | 147.7607 | 72.452 | 60.983 |
| | RMSE | 0.1577 | 7.643 | 8.679 |
| | CC | 0.956 | 0.851 | 0.712 |
| 0.06 | PSNR (dB) | 147.8030 | 73.543 | 65.673 |
| | RMSE | 0.1574 | 7.256 | 8.034 |
| | CC | 0.964 | 0.823 | 0.698 |

a modified Shannon entropy function. The elimination of speckle noise has been proved and compared with the image metrics.

Table 2 shows a comparison of the proposed filter with the circular spatial filter in spatial domain and a wavelet filter with Bayes function in wavelet domain. The values of the proposed filter shown above for comparison have taken into account only the results obtained for probability of maximum intensity pixel. The results illustrated below clearly explain that the proposed filter has a better performance than the filters under comparison. The peak signal-to-noise ratio (PSNR) of the proposed filter has a remarkable increase which shows that the noise in the image is removed in a profound way. The root mean square error (RMSE), which has to be reduced, is comparatively high in the other two filters. The correlation coefficient (CC), which exhibits the correlation between the input image and the filtered image, acts as a tool to verify that the anatomical details are preserved.

The proposed filter shows a close correlation, whereas the filters under comparison do not have a close correlation. As mentioned, the wavelet domain filters are application specific and are not suitable for all cases. The circular spatial filter is suitable only for high noise levels, whereas the proposed filter exhibits a constant range of image metrics for all range of noise levels.

Figures 31 and 32 show the apical four-chamber view of hypertrophic cardiomyopathy with the output of the proposed filter and circular spatial filter, respectively. The proposed filter presents the output in a more feasible way than the circular spatial filter.

Figures 33 and 34 exhibit the parasternal short axis view of aortic stenosis with output of proposed filter and wavelet filter with Bayes function, respectively. The output of the wavelet filter is missing the image clarity, which predicts that the wavelet filter is not suitable for the diagnosis of the mentioned heart diseases. The output of the wavelet filter is also missing the related features present in the image, whereas those features can be clearly witnessed in the proposed filter output.

The circular spatial filter and the wavelet filter using Bayes shrinkage function failed in providing information regarding

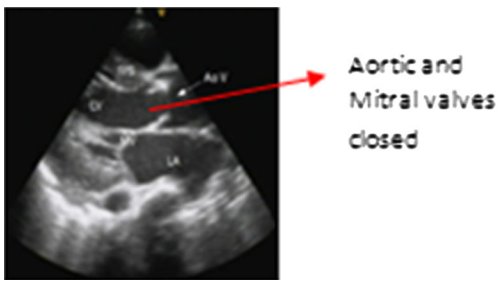


**Fig. 30** Output of the proposed filter

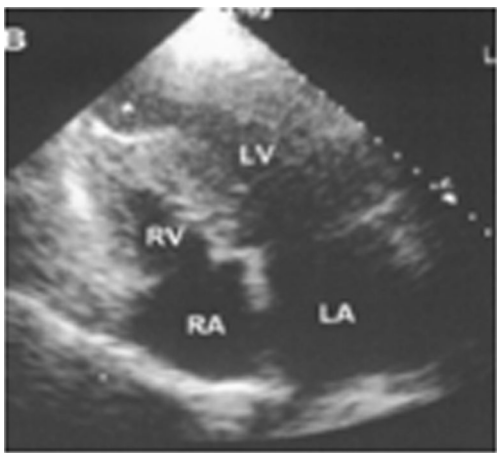


**Fig. 31** Output of the proposed filter

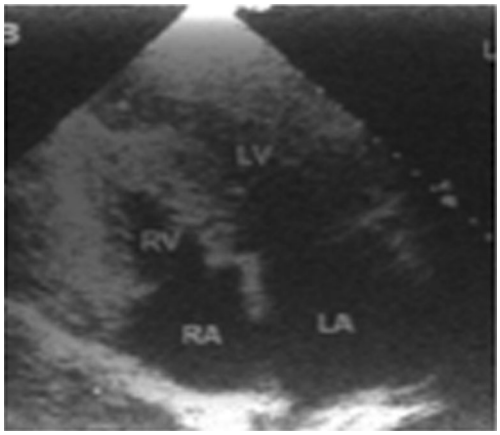


**Fig. 32** Output of the circular spatial filter


**Fig. 33** Parasternal short axis view of aortic stenosis with output of proposed filter

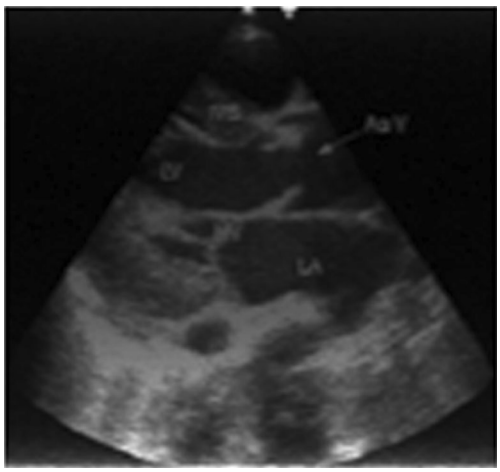


**Fig. 34** Parasternal short axis view of aortic stenosis with output of wavelet filter with Bayes function

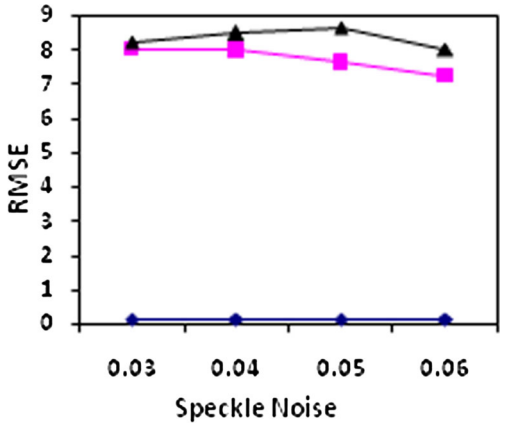


**Fig. 35** Comparison of RMSE

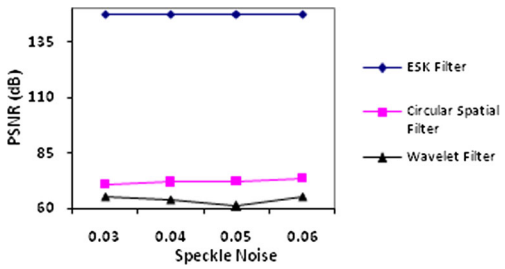


**Fig. 36** Comparison of PSNR (dB)

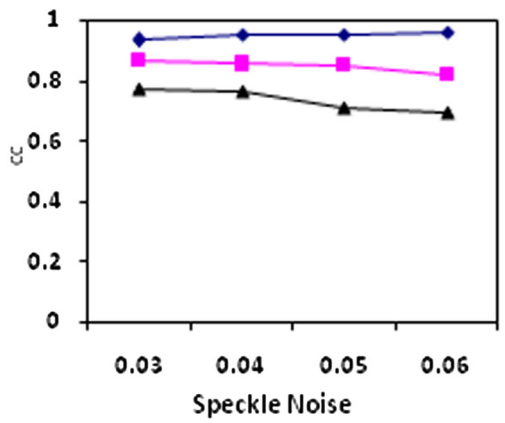


**Fig. 37** Comparison of CC

the edges and aortic and mitral valves of the heart. It is clearly evident from the results that, as the noise level increases, the performance of the wavelet filter using Bayes shrinkage function declines very sharply, whereas the proposed filter endows with an enhanced output for diseases, namely hypertrophic cardiomyopathy and aortic stenosis, in spite of the changes in the noise. The circular spatial filter is not suitable for low levels of noise. The correlation coefficient (CC) of the proposed filter shows a close relationship (Table 2) between the original image and the output of the proposed filter image, whereas a reduction in the correlation is notified in the circular spatial filter image and the wavelet filter using Bayes shrinkage function.

Figures 35, 36, and 37 show the graphical comparison of RMSE, PSNR (dB), and CC of the proposed filter compared with circular spatial filter and wavelet Filter. The proposed filter (entropy-based straight kernel (ESK) filter) shows a better performance than the circular spatial filter and wavelet filter. It exhibits that, for the wavelet filter using Bayes shrinkage function, PSNR decreases for increase in noise level and RMSE increases for increase in noise. As mentioned, PSNR of the circular spatial filter is better for high levels of noise than lower levels. The root mean square error approximately is maintained a constant for the entropy-based straight kernel filter (proposed filter). The CC of the proposed filter shows a close correlation between the original image and the filtered image. This means that the proposed filter has retained the anatomical facts without blurring of the original details, whereas the other two filters have reduced in their CC. The proposed filter outperforms and provides a stable output, irrespective of changes in noise without compromising the structural data.

## Conclusion

The proposed method is verified with approximately 36 echocardiography images. A sample result for apical four-chamber view image of a normal heart, apical four-chamber view of hypertrophic cardiomyopathy, and parasternal short axis view of aortic stenosis images are presented in this paper. The proposed method has proven to be outstanding with respect to the objective fidelity criteria, namely, PSNR, RMSE, and CC. The paper has illustrated the constant performance of the proposed filter with respect to the level of speckle noise. It can be witnessed that the proposed filter performs in an optimal manner for all levels of noise when compared to circular spatial filter and wavelet filter using Bayes shrinkage function. There is no uncertainty in the performance of the proposed filter, which has enhanced the quality of the echocardiography image, without blemishing the characteristics of the image and also illuminating the latent anatomy of the heart. Thus, the proposed filter is more suitable for the diagnosis of the relevant parameters needed for aortic stenosis and hypertrophic cardiomyopathy. In the future, the method can be implemented for any ultrasound images and the results can be verified.

**Acknowledgments** The authors would like to thank Dr. S. Murugapandiyan, Pranav Hospital, Salem, for his kind support in rendering the required echocardiography images.

## References

1. Milkowski A, Y Li, D Becker, Syed O. Ishrak: “Speckle reduction imaging”, GE Medical Systems, Ultrasound, 2004
2. Hou Z, Yau WY: ‘Visible entropy: a measure for image visibility’, International Conference on Pattern Recognition, IEEE Computer Society. IEEE Trans Sonics Ultrason 30(3):156–163, 2012
3. Mateo JL, Fernández-Caballero A: Finding out general tendencies in speckle noise reduction in ultrasound images. Expert Syst Appl 36: 7786, 2009. Science Direct
4. Chen Y, Broschat S, Flynn PJ: Phase insensitive homomorphic image processing for speckle reduction. Ultrason Imaging 18:122–139, 1996
5. Benzarti F, Hamid Amiri: “Speckle noise reduction in medical ultrasound images”, International Journal of Computer Science Issues, Vol 9, Issue 2, No 3, ISSN 1694-0814, 2012
6. Kanithi AK, Meher S: Study of spatial & transform domain filters for efficient noise reduction”. Doctoral Dissertation, National Institute of Technology, Rourkela, India, 2008
7. Astola J, Kuosmanen P: Fundamentals of nonlinear digital filtering. CRC, Boca Raton, FL, 1997
8. Chen T, Ma KK, Chen LH: Tri-state median filter for image denoising. IEEE Trans Image Process 8:1834–1838, 1999
9. Perona P, Malik J: Scale-space and edge detection using anisotropic diffusion. IEEE Trans Pattern Anal Mach Intell 12(7):629–639, 1990
10. Krissian K, Westin CF, Kikinis R, Vosburgh K: Oriented speckle reducing anisotropic diffusion. IEEE Trans Image Process 16(5): 1412–1424, 2007
11. Lee JS: Digital image enhancement and noise filtering by use of local statistics. IEEE Trans Pattern Anal Mach Intell PAMI-2(2):165–168, 1980
12. Frost VS, Stiles JA, Shanmugan KS, Holtzman JC: A model for radar images and its application to adaptive digital filtering of multiplicative noise. IEEE Trans Pattern Anal Mach Intell 4(2):157–166, 1982
13. Tomasi C, Manduchi R: “Bilateral filtering for grey and color images, ” Proceedings of IEEE international conference on computer vision, pp. 839- 846,1998
14. Buades A, Coll B and Morel J: “A non-local algorithm for image denoising,” Proc. IEEE international conference on computer vision and pattern recognition, pp. 60-65,2005
15. Suganya Devi S, Suganya Devi, D: “Find filtering techniques for eliminating speckle noise in ultrasound medical images via image cleaning algorithm”, International Journal of Computer Science and Management Research, Volume 1, Issue 2, September 2012, ISSN 2278-733X, 2012
16. Vijayarajan R, Muttan S: Cross neighbourhood kernel filtering for speckle noise removal in ultrasound images. Int J Recent Technol Eng 1(2):2277–3878, 2012. ISSN
17. Bhoi N, Meher S “Circular spatial filtering under high noise variance conditions,” Computers & Graphics, Elsevier, vol. 32, no. 5, pp. 568-580, 2008
18. Donoho DL, Johnstone IM: Ideal spatial adaptation via wavelet shrinkage. Biometrika 81(3):425–55, 1994

19. Donoho DL, Johnstone IM: Adapting to unknown smoothness via wavelet shrinkage. J Am Stat Assoc 90(432):1200–1224, 1995
20. Luisier F, Blu T, Unser M: A new SURE approach to image denoising: interscale orthonormal wavelet thresholding. IEEE Trans Image Process 16(3):593–606, 2007
21. Chang S, Yu B, Vetterli M: Adaptive wavelet thresholding for image denoising and compression. IEEE Trans Image Process 9(9):1532–1546, 2000
22. Chen GY, Bui, TD, Krzyzak A: "Image denoising using neighboring wavelet coefficients", proceedings of IEEE international conference on acoustics, speech and signal processing '04, pp. 917-920, 2004
23. Mastriani M, Giraldez AE: "Smoothing of coefficients in wavelet domain for speckle reduction in synthetic aperture radar images", Journal of Graphics Vision and Image Processing, vol. 7(special issue), pp.1-8, 2007
24. Vishwa A, Sharma S: "Speckle noise reduction in ultrasound images by wavelet thresholding", International Journal of Advanced Research in Computer Science & Software Engineering, Volume 2, Issue 2, ISSN 2277 – 128X,2012
25. Kang SC, Hong SH: Experimental and theoretical analysis of wavelet based denoising filter for echocardiographic images. Press, Amsterdam IOS, 2001
26. Rajalaxmi S, Nirmala S: "Echocardiographic image denoising & objective fidelity criteria estimation using entropy paramounted linear regression filter", IEEE Conference Proceedings on Emerging Trends in Science, Engineering & Technology, ISBN 978-1-4673-5141-6, 2012
27. Kalaivani Narayanan S, Wahidabanu RSD: 'A view on despeckling in ultrasound imaging', International Journal of Signal Processing, Image Processing and Pattern Recognition Vol. 2, No.3, 2009
28. Michailovich O, Tannenbaum A: De-speckling of medical ultrasound images. IEEE Trans Ultrason Ferroelectr Freq Control 53(1):64–78, 2006
29. Thangavel K, Manavalan R, Aroquiaraj L: Removal of speckle noise from ultrasound medical image based on special filters: comparative study. ICGST-GVIP J 9(3):25–32, 2009
30. Zhou Wang, Bovik AC: 'A universal image quality index', IEEE Signal Processing Letters, 2002